

EVALUATION OF BIOFIDELITY OF ECE REGULATION NO. 22 INJURY CRITERIA

Paul Rigby
Brett Juhas
Jessica Wong
Philemon Chan
L-3/Jaycor, San Diego CA
USA

Paper Number 11-0366

ABSTRACT

The biofidelity of the injury criteria of the European standard for motorcycle helmets (ECE Regulation No. 22, Section 7.3 Impact-absorption tests), were examined against biomechanically based injury metrics. Using a method to measure the helmet contact pressure on the headform during impact, twenty helmets were dropped according to ECE R22 free drop specifications. A total of 76 impacts to the front, crown, rear, right and left side of the helmet were examined using finite element simulations to predict skull fracture. The ECE R22 criteria, peak head acceleration and HIC, were correlated with these injury metrics.

It was found that ECE R22 criterion of peak headform acceleration is the best correlate with all injuries. HIC was an acceptable correlate for brain injury metrics but a very poor correlate to skull strain. The current peak headform acceleration limit of 275 g resulted in a 20% probability of skull fracture.

This research has shown that peak head acceleration can be an acceptable injury metric for skull fracture using the ECE R22 test method. The current ECE R22 linear acceleration limit of 275 g is slightly higher than the calculated thresholds of injury used in this study for skull fracture, 252 g for 15% probability of skull fracture. Even though a free head drop method was used, the resultant translational acceleration trace at the center of gravity of the headform proved no better at predicting concussion than the rigidly mounted FMVSS No. 218 headform. When headform rotation was measured and used in the SIMon analysis, an increase in the concussion injury metric was seen. In order to use SIMon as a brain injury analysis tool, unconstrained free drops with headforms instrumented to record angular motion are necessary.

A comparison of test results for helmets which were tested using both FMVSS No. 218 and ECE R22 methods was conducted. It was found that the peak

head acceleration was an acceptable injury metric for skull fracture in both studies. Although FMVSS No. 218 and ECE R22 test protocols are different, both have a pass/fail criterion based on the peak head acceleration. Since peak head acceleration correlates to skull fracture, any future modification of the peak head acceleration criterion can be based on acceptable probability of skull fracture analysis.

INTRODUCTION

The National Highway Traffic Safety Administration (NHTSA) of the US Department of Transportation (DOT) estimated that motorcycle helmet use has increased from 48 percent in 2005 to 67 percent in 2009 (NHTSA 2009). However, in a 2007 NHTSA report, it was found that a motorcyclist is 34 times more likely to die than a person riding in a car. By wearing a helmet the likelihood of death decreases by 37 percent. In total cost, NHTSA has estimated that wearing a motorcycle helmet has saved \$1.3 billion dollars in medical expenses in 2002 alone (NHTSA 2007). If everyone that was injured was wearing a helmet, a further \$835 million would have been saved.

The objective of this study was to evaluate the biomechanical basis of the impact absorption requirements of United Nations Economic Commission for Europe (ECE) Motorcycle Helmet Regulation No. 22.05 versus known biomechanically-based injury criteria in the context of the ECE R22 test protocol. This study will also compare the biofidelity results with that of a previous study investigating the biofidelity of the U.S. helmet standard FMVSS No. 218.

ECE R22 Motorcycle Helmet Standard

The latest revision of ECE R22 was adopted in 2000. ECE R22 requires impact absorption, friction, rigidity, and retention system tests. This study will focus on the impact absorption test.

Impact-Absorption Test The underlying principle of the impact-absorption test is to “determine by recording against time the acceleration imparted to a headform fitted with the helmet, when dropped in guided free fall at a specific impact velocity upon a fixed steel anvil” (UNECE R.22 2000). To perform this test, the helmet is fitted to an ISO full faced headform. The ISO headform is defined by the EN960 standard. A single triaxial accelerometer is mounted at the center of gravity of the headform.

Unlike FMVSS No. 218 in which the headform is firmly attached to the rail, ECE R22 uses a free fall system that allows the helmet to freely move during impact. The helmet is set on a mobile system which supports the helmeted headform during free fall. The support system can either be guided using wires or attached to a rail system.

There are two types of anvils used, a flat steel anvil with a flat impact face (130 mm diameter) and a steel kerbstone anvil (Figure 1). The impact velocity against either anvil is 7.5 (+0.15 / -0.0) m/sec. The velocity of the moving mass is measured between 1 and 6 cm before impact and must be accurate within 1%.

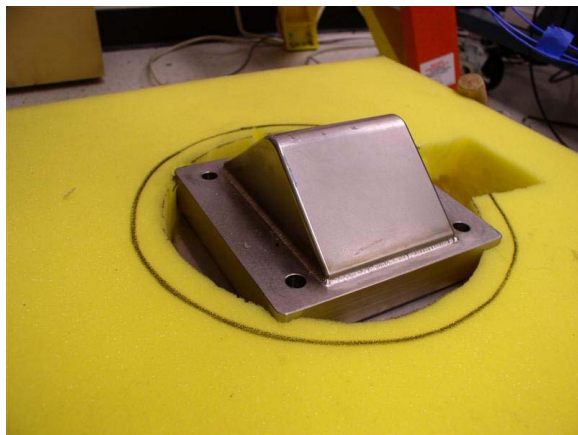


Figure 1. Kerbstone anvil used in ECE R22

Each helmet is impacted in four locations; the front (B), either side (x), rear (B) and crown (P). Each location is only hit one time. ECE R22 specifies the front visor to be impacted, however this was not performed for this study. The ECE R22 protocol also calls for impacts under ambient, heated, low temperature and ultraviolet radiation and moisture conditions. Each condition has an anvil type associated with it. Drops were restricted to ambient temperatures for this study (temperature $25^{\circ}\text{C} \pm 5^{\circ}\text{C}$, relative humidity $65\% \pm 5\%$ for four hours).

To pass the impact-absorption requirement of ECE R22, the criteria

$$A_{\max} \leq 275 \text{ g, and} \\ \text{HIC}_{36} \leq 2400,$$

must be satisfied for all drops on the helmet. A_{\max} is the peak resultant acceleration of the headform. HIC is calculated as the maximum of the equation

$$\text{HIC} = \left[\frac{1}{t_2 - t_1} \int_{t_1}^{t_2} a(t) dt \right]^{2.5} (t_2 - t_1)$$

where a is the resultant acceleration in g and t_1 and t_2 are any two points in time during the impact.

HIC was developed in 1971 from modifications of the Wayne State University Tolerance Curve and Gadd Severity Index (Newman 1980). HIC was incorporated into FMVSS No. 208 and is widely used in the automobile industry. HIC is calibrated to be used with an unhelmeted Hybrid III head and as such does not characterize any one particular type of injury, but is a general measure for head injury. A HIC_{15} of 700 correlates to a 11% probability of an AIS 3+ injury (NHTSA 2008). When investigating how HIC correlates to a specific head injury criterion, Vander Vorst et al. (Vander Vorst, Stuhmiller et al. 2003) demonstrated that HIC correlates poorly with skull strain due to its high sensitivity to target compliance. Although, when the contact area is considered, HIC correlates well with strain. It is unknown how a helmet affects the HIC injury-risk function. It is also unknown how using a rigid metal headform instead of a Hybrid III head affects HIC.

The authors could not find documentation showing how the ECE R22 criteria of 275 g peak head acceleration and HIC_{36} of 2400 was decided upon. In March 1995, the original ECE Regulation No. 22 was amended to add in the 275 g and HIC_{36} of 2400 criteria. Previous to this amendment, ECE R22 drop tests were done at 7.0 and 6.0 m/s (depending on the anvil) with the following criteria, “the resultant acceleration measured at the centre of gravity of the headform is less than 150 g for any 5 msec continuously and at no time exceeds 300 g.” FMVSS No. 218 is structured similarly in that it contains requirements limiting the dwell time of acceleration over 150 g to 4.0 msec and acceleration over 200 g to 2.0 msec.

For skull fracture, ECE R22 will be compared against the generalized linear skull fracture criteria. Vander Vorst (Vander Vorst, Stuhmiller et al. 2003; Vander Vorst and Chan 2004) first presented the linear skull fracture criteria called skull fracture correlate (SFC). SFC is the average headform acceleration over the HIC_{15} time interval. The HIC_{15} time interval is the

time duration, up to 15 msec, during which the peak HIC value is found. SFC was validated using post mortem human specimens (PMHS) data from the historical Hodgson and Thomas tests (Hodgson and Thomas 1971; Hodgson and Thomas 1973) and recent data from Medical College of Wisconsin (MCW). The PMHS data were correlated with Hybrid III headform tests and finite element model simulations. The first work (2003) demonstrated that the skull strain calculated by a finite element model (FEM), the fracture data and SFC all correlated well with one another with well defined confidence bands, hence validating the biofidelity of SFC. The following work (2004) expanded the validity of SFC to lateral impact using more newly obtained PMHS data. Chan et al. (Chan, Lu et al. 2007) developed a generalized linear skull fracture correlate using frontal and side impact PMHS data. The head impacts in this study involved side, frontal, and crown hits; therefore, the generalized SFC injury curve is used.

In the previous study on FMVSS No. 218, brain injuries were evaluated using the NHTSA SIMon finite element head model version 1 (Takhounts, Eppinger et al. 2003). It was found that driving SIMon using only translational acceleration did not produce significant injury metrics. It was concluded that both translational and rotational motion was necessary to achieve meaningful results from SIMon. Zhang et al. has shown that rotational motion contributes significantly to strain in the brain during impacts compared to translational acceleration (Zhang, Yoganandan et al. 2006). In this study, the rotation of the headform during impact and how it affects SIMon injury metrics will also be investigated. This will be achieved using a new nine accelerometer package system for the ISO headform. NHTSA released a newer version of SIMon in 2009 (Takhounts et al., 2008). The current study continued using the original version to be consistent with prior work done in evaluating the biofidelity of the injury limits in FMVSS No. 218 (Rigby et al., 2009).

METHODS

Instrumentation for Measuring Headform Pressure To predict the efficacy of a particular helmet using finite element calculations coupled with the head would require a validated structural model of the helmet. This task is impractical for each helmet model to be tested. However, if during a drop test, the pressure applied by the helmet to the headform were measured, and this pressure applied to the anatomical finite element model to compute the skull strain, then the

probability of skull fracture could be predicted for the specific helmet. To accomplish this, instrumentation to measure the pressure contours on the headform was developed.

TekScan's FlexiForce sensors were chosen to measure the contact pressure between the helmet liner and the headform. Extensive tests were conducted to characterize the FlexiForce force sensors. The sensors were found to have acceptable drift, repeatability, and linearity when a normal force was applied. A drop in signal voltage was observed when the sensor was subjected to shear force. This negative voltage was proportional to the normal force acting on the sensor and was repeatable.

During the impact absorption test, the FlexiForce sensors attached to the headform would be subjected to shear forces, causing error in the experimental data. In order to get the true force from the sensors, the shear force experienced by the sensors was reduced by applying petroleum jelly directly to each FlexiForce sensor and then covering them with Teflon strips. Once the best method for reducing shear error was found, an array of sensors was glued to a Cadex (type J) medium size ISO headform. The sensors were attached using silicon adhesive sealant then the petroleum jelly and Teflon strips were applied. A total of 36 FlexiForce sensors were used to cover the impact area of the headform. A fully treated and instrumented headform is shown in Figure 2.

The FlexiForce sensors were distributed in a regular grid pattern, and it was assumed that the pressure measured by a sensor was uniform over the sub-grid area with the sensor at the center. For each impact configuration (crown, right side, left side, back, or frontal drop), it was assumed that the contact load would primarily be borne by the impact side of the headform and tangential loads were negligible. Therefore, the sensors were placed only out to the edge of the impact side of the headform. The total impact area was estimated for each impact configuration and distributed evenly to each sensor sub-grid area for inputs to the anatomical finite element model for skull fracture prediction.



Figure 2. Fully instrumented headform for crown drops.

Impact Absorption Tests One hundred drop tests were conducted to gather input data for the finite element model simulations. Impact absorption tests were performed according to specifications given in the ECE R22 document. The helmets were dropped in a guided free fall onto either a flat or a kerbstone anvil at a speed of 7.5 m/sec (ECE R22 Sec# 7.3). Half the tests were conducted against the flat anvil; the other half used the kerbstone anvil. There were four impact sites selected for each helmet: crown, front, right and left side (ECE R22 Sec# 7.3.4.2).

The acceleration of the headform was measured using a triaxial accelerometer placed at the center of gravity of the headform. The anvils were bolted onto a Kistler 925M113 load cell connected to a Kistler 5118B2 power supply/coupler which was in turn bolted to the cement floor. Headform acceleration, load cell force, and FlexiForce pressure data was taken by LabView version 7.0 on a BSI FieldGo Pentium 4 computer.

Twenty helmets were used in the tests. Helmet types consisted of a mixture of full face helmets, open face helmets, and half helmets. All helmets were designed and certified to HMVSS No. 218. No documentation on certification to ECE R22 was found. Each helmet was struck at all five of the impact locations. For each impact location, ten helmets were randomly selected to impact the flat anvil while the other ten helmets were then impacted against the kerbstone anvil. As per ECE R22 protocol (Sec# 7.4.2.1.2.1), the chin strap on each helmet was tightened as much as possible to secure the headform so that it did not shift before impact. In order to achieve a guided free fall, the helmet/headform assembly was placed onto the aluminum ring attached to the drop tower (Figure 3). A mesh bag was secured to the ring to catch the

helmet after impact. All absorption tests were conducted at ambient conditions. The impact absorption test was the only type of test conducted; all of the other test procedures identified by ECE R22 (Sec# 7) were not done.



Figure 3. Impact absorption test setup.

Skull Fracture Finite Element Model The maximum principal skull strain was calculated for each impact absorption test using a refinement of the anthropomorphic, medical imaging-based, finite element model of Vander Vorst, et al. (Vander Vorst, Chan et al. 2004). The baseline model was composed of 24,000 elements and resolved the outer and inner tables, diploe, brain, scalp, and face. The mass of the baseline model was 4.54 kg. The skull components were modeled using fully integrated thick shells and the brain, scalp, and face were modeled with fully integrated bricks. Since this model was based on CT imaging of a PMHS, the skull shape and thickness are anatomically correct. The thickness of the compact skull tables was set to be 1 mm uniformly, since they were too thin to be resolved from the CT scan. The 1-mm value was based on measurements of photographic cross-sections from the Visible Man project (NIH 2000). The properties of the biological materials were taken from the open literature. The elastic properties of compact skull bone were from Wood (Wood 1971). Diploe was taken to be linear elastic (Khalil and Hubbard 1977). The linear viscoelastic properties of the brain were from Takhounts et al. (Takhounts, Eppinger et al. 2003). Scalp was assumed to be viscoelastic with properties calibrated by Vander Vorst et al. (Vander Vorst, Stuhmiller et al. 2003).

The sensor locations on the headform were mapped directly to the scalp elements of the skull fracture FEM (Figure 4). For example, if the headform had a line of seven sensors equally spaced from the anterior to posterior reference line, the location of the reference plane on the skull fracture FEM would be

determined and the seven sensor locations would be equally spaced similar to the headform. The maximum strain in either the inner or outer table of the skull for each test was found and used in the statistical analysis.

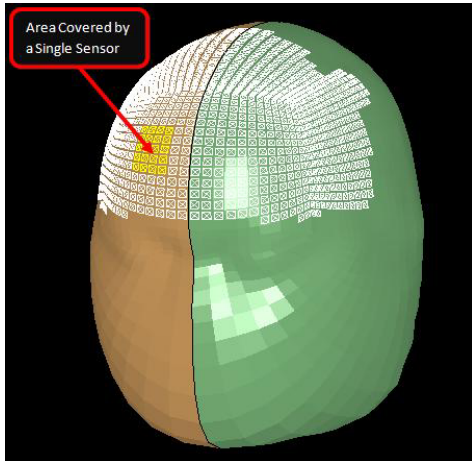


Figure 4. LS-Dyna finite element model showing the sensor locations for front impacts.

Headform Rotation Analysis In a parallel helmet study sponsored by the U.S. Army Medical Research and Materiel Command, a method for calculating the rotational motion of an ISO headform was developed. These methods from the HMSS study have been adopted into this study to more fully evaluate the ECE R22 helmet standard.

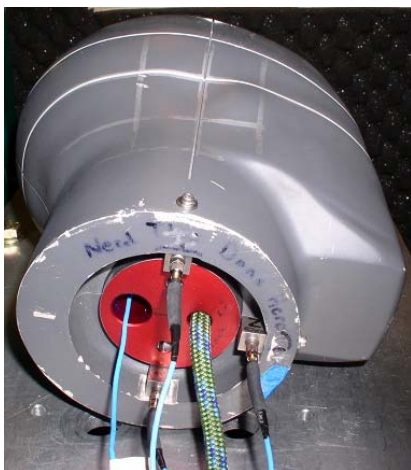


Figure 5. Picture of the headform equipped with linear accelerometers.

SIMon Methods and Results using Angular Velocity Data Four extra helmet drops were conducted on the front, crown, right and left side of a helmet using the NAP configured ISO headform in

order to determine the effect rotation during impact has on SIMon brain injury results. Two SIMon cases for run for each impact. The first case was using only the translational acceleration data taken from the CG of the helmet. This is the same method used when examining ECE R22 in this study. The second case was to use both the translational acceleration and the rotational velocities for each impact. The three SIMon injury metrics (CSDM, DDM, and RMDM) were then plotted against each other in order to observe the effect of rotation.

Each test was computed out to 20 msec. Although helmets continued to move after 20 msec, both the translation and rotational acceleration due to the impact were over. The injury measures recorded were: cumulative strain damage measure (CSDM), dilatational damage measure (DDM), and relative motion damage measure (RMDM). SIMon reports CSDM values at various tolerances of strain. Takhounts et al., reports that a CSDM with a tolerance of 15% strain in the brain achieved the best correlation with diffuse axonal injuries compared to other tolerances. Therefore, CSDM with a tolerance of 15% strain was used in this study. The RMDM threshold for injury was established using only sagittal impact data. Data from side hits were not used to evaluate RMDM, only crown, front and rear impact results are reported as suggested in the SIMon documentation.

RESULTS

Impact Attenuation Tests A total of 20 helmets were used in this study. Each helmet was dropped once on the crown, front, right side, left side, and back in locations specified by ECE R22 protocol. Out of the 80 impacts performed, 59 tests were used in analysis. This was split up between 14 crown hits, 17 front hits, 14 right and 14 left side hits. A test was removed if 1) there was a misfire of the data acquisition trigger and the data for the drop was not recorded, 2) if it was found that more than 3 FlexiForce sensors were broken during impact, or 3) if the impulse of the head computed with the FlexiForce was more than 50% off from that calculated using the headform accelerometer. The majority of the tests removed were due to misfires of the data acquisition software.

Thirty percent of the helmets passed the current criteria for ECE R22. Helmets that failed to pass, failed both the peak acceleration limit and the HIC limit for the majority of the cases. There was significantly more failures when the flat anvil was used compared to the kerbstone anvil. For all drops

combined, drops against the flat anvil had a 47.5% pass rate and drops against the kerbstone anvil had an 87.5% pass rate. There was not a single case where identical helmets passed on a flat anvil but failed on the kerbstone anvil. However, there are multiple cases where identical helmets failed on a flat anvil but passed on the kerbstone. The majority of the failures happened on the crown against the flat anvil, achieving a 20% pass rate.

Since the FlexiForce sensors did not cover the entire contact area between the helmet and the headform, it was unknown if the sensors would pick up the entire load delivered to the headform. In order to determine if the correct loading was applied, the FlexiForce force data was validated against the headform accelerometer data. The total vertical component of the force from the FlexiForce sensors was computed and divided by the mass of the headform to get the resultant head acceleration. Each FlexiForce sensor was assumed to cover both its area and a portion of the surrounding area. This provided complete surface area coverage in the finite element model. The impulse of the headform was also calculated using both the FlexiForce and accelerometer data (Figure 6).

If the measured accelerometer impulse and the calculated FlexiForce impulse were not equal, a factor was applied to the FlexiForce pressures to preserve the accelerometer measured impulse at the peak acceleration. This was to assure a conservation of impulse between the acceleration data and the FlexiForce data. Since the FlexiForce sensors were assumed to cover its own area and the area around it the impulse calculated from the FlexiForce sensors could be slightly off, especially if only a few sensors recorded the majority of the impact force. This impulse factor ranged from 0.80 to 1.50 with an average of 1.17. This factor was applied to the pressures at each sensor for the finite element calculations. The headform acceleration and impulses data measured by the accelerometer and those calculated from the scaled FlexiForce data were in good agreement, as shown in Figure 6. All FEM calculated peak head acceleration values were within 10% of the experimental values.

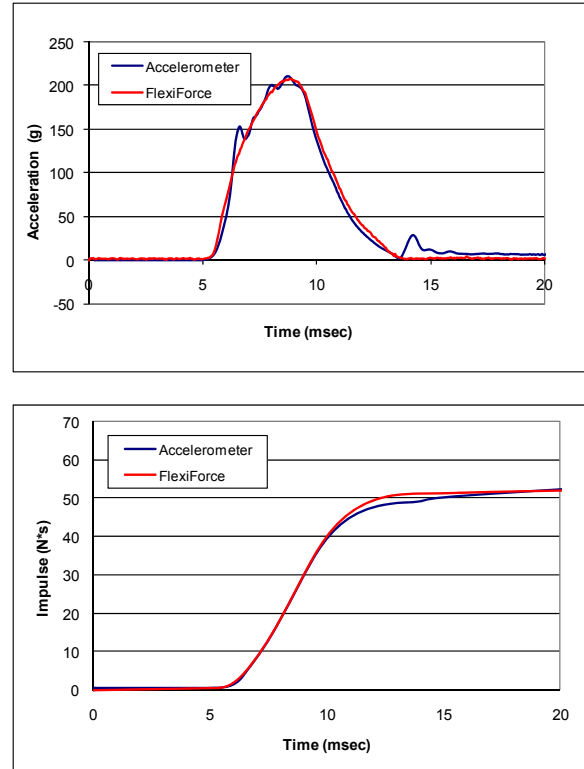


Figure 6. Head Acceleration and Impulse Data Comparison

Skull Fracture Evaluation A finite element simulation was performed for each impact attenuation test which passed the headform impulse criterion. The FlexiForce pressure measurements were used as inputs in to the model. Each simulation was analyzed out to 20 msec. After the drop simulation was completed, the maximum principle strain in either the outer or inner table of the skull was determined. The peak strain for the test was determined by averaging the strain-time history of the element in the model with the peak strain with all of its neighbors. By averaging a group of elements, single element anomalies can be avoided. The headform acceleration was also calculated by the FEM and compared to the experimental values. In each case, the FEM-calculated head acceleration trace closely matched the experimental results. Characteristic contour plots of the pressure applied to the scalp and the resulting pressure transmitted to the skull are shown in Figure 7.

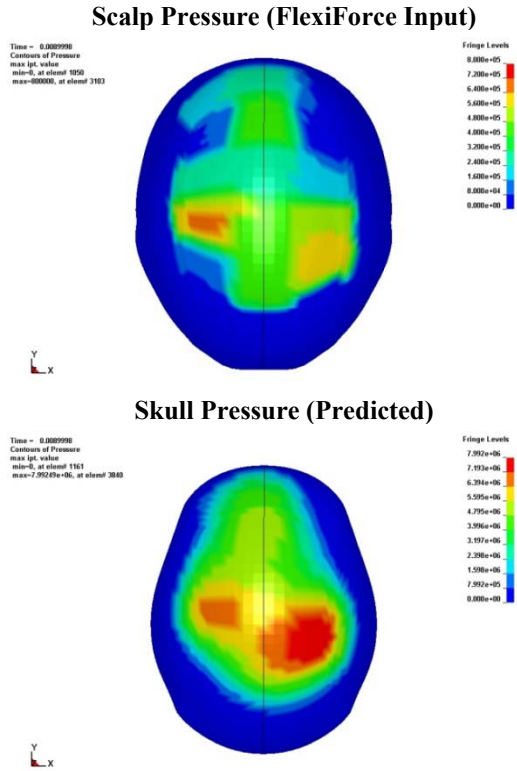


Figure 7. Pressure Contour Plots of Scalp and Skull

The finite element model did not reach the termination time of 20 msec for a few of the side impact cases. This was due to excessive deformation of the scalp from the very high pressures recorded during these drop tests. In these cases, the model was run out until failure and the last recorded skull strain was used. Failure usually occurred within a millisecond of the peak input pressure; therefore, it was assumed that the strain values are close to the actual values.

An adjustment of the SFC risk curve for the rigid ISO EN960 full faced headform was made using the finite element results. The standard SFC risk curve was originally established for the Hybrid III headform with an outer rubber skin, with 15% probability of skull fracture predicted by SFC=124 g (Chan, Lu et al. 2007), but this value will change for the rigid headform with no skin. Fortunately, skull fracture can be predicted using the skull strain calculated from the anthropomorphic FEM. Therefore, the SFC risk curve was adjusted for the ISO full faced headform by correlating the SFC values calculated from the headform acceleration with the skull strain calculated from the FEM (Figure 8). For 15% probability of skull fracture, which corresponds to 0.19% of skull strain, the SFC value will be 189 g for the ISO full

headed headform. However, as can be seen in Table 1, the correlation for all ECE R22 tests combined was $R^2=0.39$. This is lower as compared to the correlation observed in the previous Rigby and Chan FMVSS No. 218 study ($R^2 = 0.66$). Different from the FMVSS No. 218 study where correlation was relatively consistent in the three drop conditions with R^2 values of 0.48, 0.65 and 0.69, there was a much broader range of R^2 values in the current study with values as low as 0.39 in left side drops to 0.81 in crown drops.

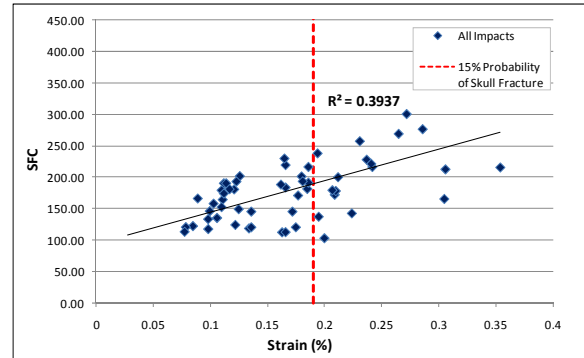


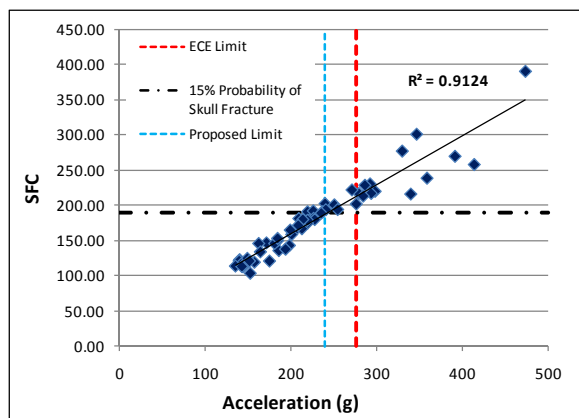
Figure 8. Correlation between SFC and Skull Strain for ISO Headform

Table 1. Strain Correlates

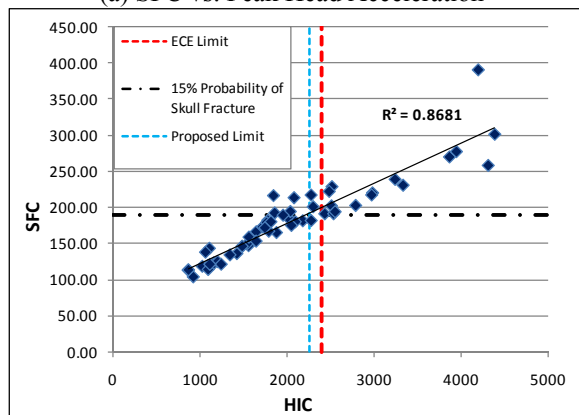
Condition	Strain vs. Acceleration			
	22-05		218	
	R^2	15% Prob Value	R^2	15% Prob Value
All	0.518	251.790	0.675	208.155
Left Side	0.555	202.660	0.738	274.929
Right Side	0.822	213.734		
Front	0.513	297.923	0.507	262.954
Crown	0.904	310.897	0.638	178.827
Condition	Strain vs. SFC			
	22-05		218	
	R^2	15% Prob Value	R^2	15% Prob Value
All	0.394	189.448	0.656	149.793
Left Side	0.392	166.296	0.690	193.325
Right Side	0.530	167.431		
Front	0.463	225.555	0.476	200.670
Crown	0.813	218.241	0.651	128.219

Condition	Strain vs. HIC			
	22-05		218	
	R ²	15% Prob Value	R ²	15% Prob Value
All	0.213	2576.84	0.616	1417.152
Left Side	0.043	2506.36	0.690	1923.354
Right Side	0.415	1672.34		
Front	0.500	3205.50	0.425	2115.330
Crown	0.795	3034.14	0.627	2258.890

SFC Correlation Using the ECE R22 injury criteria, peak head acceleration and SFC have a correlation value of $R^2 = 0.91$ (Figure 9a). SFC and HIC have a correlation value of $R^2 = 0.87$ (Figure 9b). Using the adjusted SFC for 15% probability of skull fracture of 212 g, an adjusted peak acceleration of 238 g is given. A HIC of 2265 g would correspond to a 15% probability of skull fractures based on the SFC limit of 189 g.



(a) SFC vs. Peak Head Acceleration

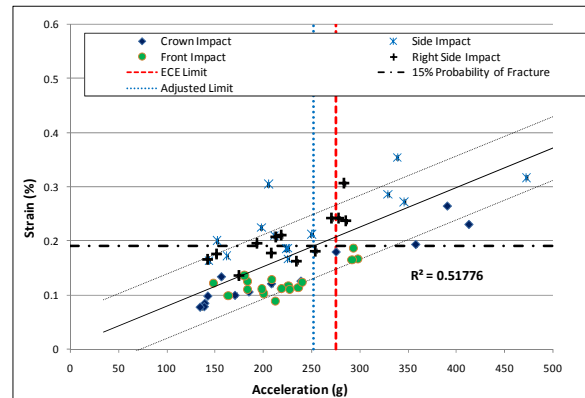


(b) SFC vs. HIC.

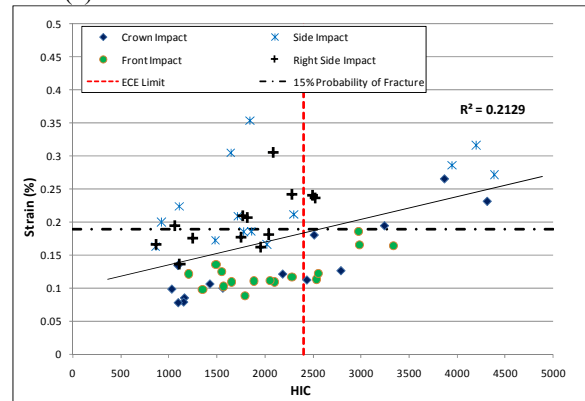
Figure 9. SFC comparison.

Strain Correlation The correlation of peak head acceleration and peak skull strain was $R^2 = 0.52$. However, the correlation was higher when looking at

individual drop conditions with R^2 ranging from 0.51 in frontal drops to 0.90 in crown drops (Table 1). However, if the linear regression is banded by one standard deviation limits, 83% of the data points are within one standard deviation error. Using the linear regression equation, a peak head acceleration of 252 g correlates to a 15% probability of skull fracture. This acceleration limit is close to the 238 g value based on the SFC comparison. The correlation between HIC and peak skull strain was $R^2 = 0.22$. Given the low correlation between peak strain and HIC, no adjusted HIC limit was determined (Figure 10).



(a) Skull Strain vs. Peak Head Acceleration



(b) Skull Strain vs. HIC

Figure 10. Skull Strain Comparison

HIC Correlation The correlation between HIC and peak head acceleration is $R^2 = 0.82$ as seen in Figure 11. The ECE R22 HIC limit of 2400 g corresponds to a peak head acceleration of 261 g.

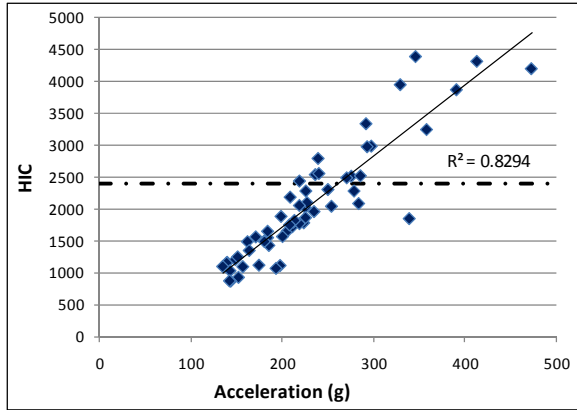


Figure 11. HIC Comparison

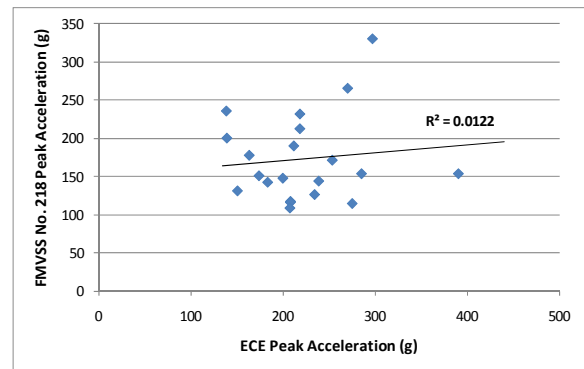
The overall results show that peak head acceleration appears to be the better correlate with the biofidelic injury metric strain, especially if impact direction is examined instead of looking at all directions as a whole. While HIC correlates well with other injury metrics (peak acceleration and SFC), it is a poor correlate to strain. A summary of the peak head acceleration comparison results are shown in Table 2, which also indicates the peak acceleration adjustments according to the published limits for the various damage measures. The current ECE R22 acceptable peak head acceleration of 275 g is slightly higher than the adjusted peak head accelerations to meet the published injury criteria for skull strain and SFC.

Table 2. Summary of Damage Measures based on Finite Element Models

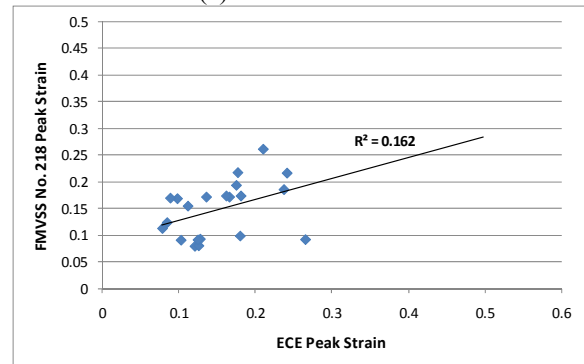
Damage Measure	Injury at 275g (ECE limit)	
	Measure	Probability
Skull Strain	0.19%	15.0%
SFC	212	33.0%
Published Injury Limit		
	Measure	Probability
Skull Strain	0.19%	15%
SFC	189	15%
Headform acceleration at published injury risk levels		
Skull Strain	252g	
SFC	238g	

Comparison to FMVSS No. 218 Helmet Study Sixteen out of the twenty helmets used in this study are the same or a very similar model helmet that was used in the previous study evaluating the biofidelity of FMVSS No. 218. The peak headform acceleration, peak strain, and HIC values computed in this study were plotted against the values determined in the FMVSS No. 218 study to determine any correlation between the standards. It

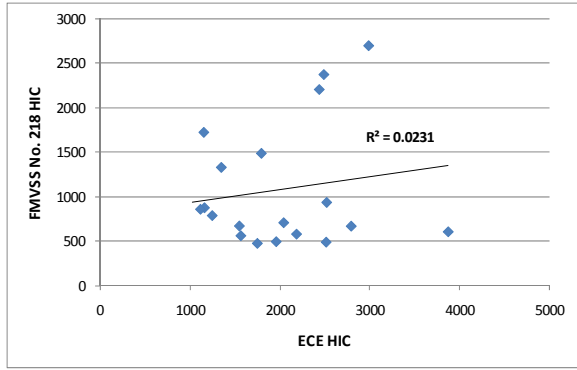
must be noted that helmets in the FMVSS No. 218 study were dropped at 6.0 and 5.2 m/s against flat and hemispherical anvils, respectively. Helmets in the ECE R22 study were dropped at 7.5 m/s against flat and kerbstone anvils. FMVSS No. 218 helmets were also dropped twice at the same location compared to once in the ECE R22 study. The injury metrics from the FMVSS No. 218 study are plotted against the same helmet's injury metrics from the ECE R22 study in Figure 12. Although FMVSS No. 218 requires two drops on the same location, only the first impact was used with ECE R22 comparison. No injury metrics show correlation between FMVSS No. 218 and ECE R22 for drops on the same helmet. This is probably due to the significant differences between headforms, test apparatus and testing protocol. FMVSS No. 218 uses a DOT half headform that is rigidly mounted to the drop tower assembly. ECE R22 used an ISO full faced headform that is dropped and allowed to freely bounce upon impact. While both protocols impact against flat anvils, FMVSS No. 218 tests against a hemispherical anvil and ECE R22 tests against a kerbstone anvil. ECE R22 also has a higher impact velocity than FMVSS No. 218. The combination of differences results in injury criteria which are not able to be correlated between the two standards.



(a) Peak Acceleration



(b) Peak Strain



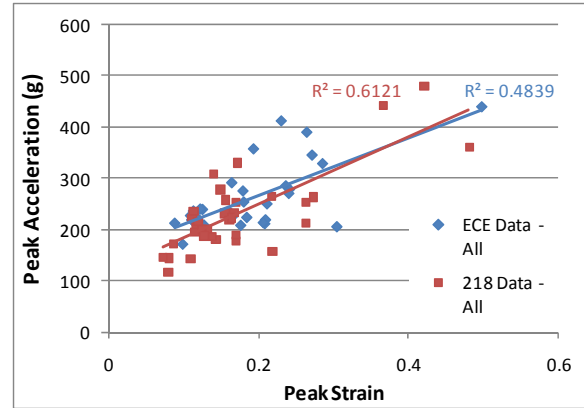
(c) HIC

Figure 12. Comparison of ECE R22 and FMVSS No. 218 Results

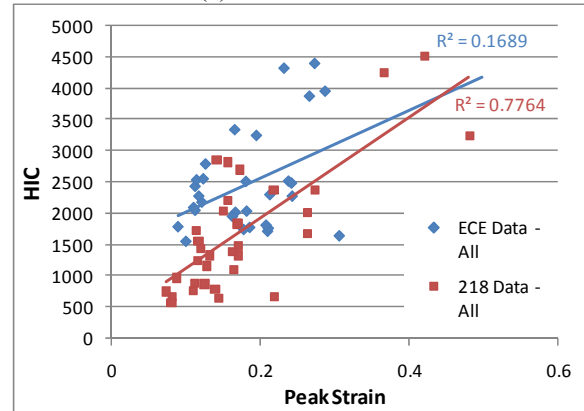
One commonality between the ECE R22 and FMVSS No. 218 tests were the use of a flat anvil. Of the helmets that were used in both studies, a comparison of data where drops were made against flat anvils was conducted to determine if the trends of both experimental methods agree. For both studies, helmets were randomly assigned to impact a flat or non-flat anvil for each impact direction. Due to the small number of helmets that fit the criteria of being used in both studies and impacted in the same orientation on a flat anvil, a comparison of the linear regression trend for all impacts against the flat anvil for both studies was conducted.

As seen in Figure 13a, the peak strain vs. peak acceleration trend line for both the FMVSS No. 218 study and the ECE study are similar. The ECE linear regression equation is $y = 560.06x + 153.93$, while the FMVSS No. 218 linear regression equation is $y = 658.51x + 117.36$. The similarity of slopes and a slight offset in the y-intercept demonstrates that when a common impact surface is employed, both test methodologies predict very similar peak strains.

Figure 13b shows that there is a difference in the trends between HIC and peak strain for the two standards. The ECE R22 trend predicts a higher HIC value and the same strain percentage when compared to the FMVSS No. 218 data. Also the correlation coefficient of $R^2 = 0.1689$ is much lower than that of the FMVSS No. 218 study.



(a) Peak Acceleration



(b) HIC

Figure 13. Comparison of correlation trends using only flat anvil data

SIMon Results using Rotational Data

Four drops were made separate of the previous tests conducted to evaluate ECE R22 to investigate the affect rotation has on the brain injury correlates calculated by SIMon. The drops were all conducted on different helmets with one drop to the front, one to each side and one to the crown. A sample angular velocity used as inputs for SIMon is shown in Figure 14. From this plot, it can be seen that the headform experiences a large angular velocity on side drops and little rotation from crown drops.

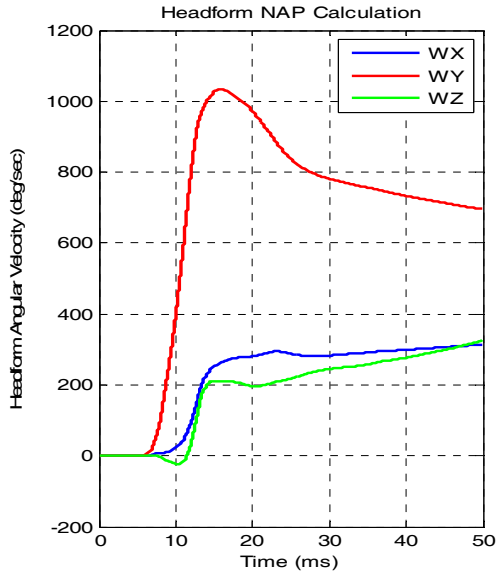
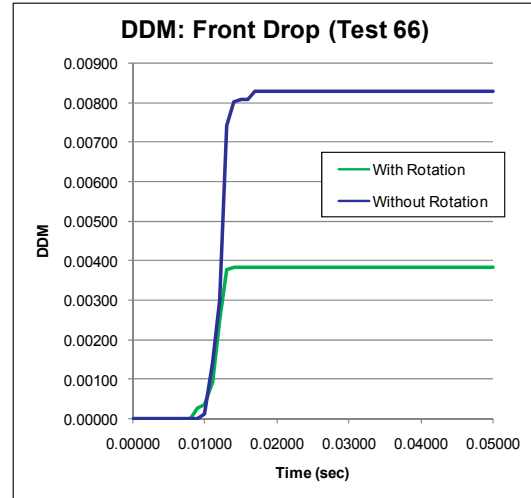


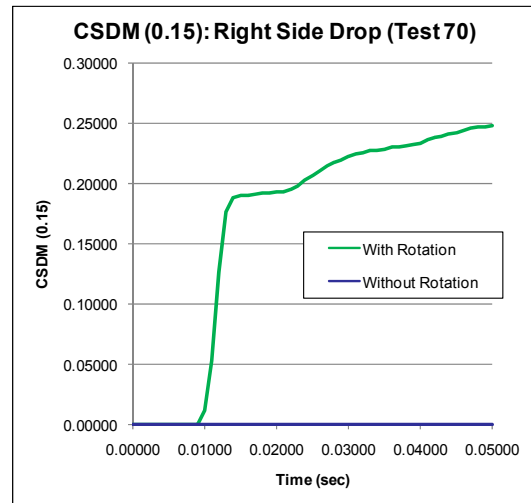
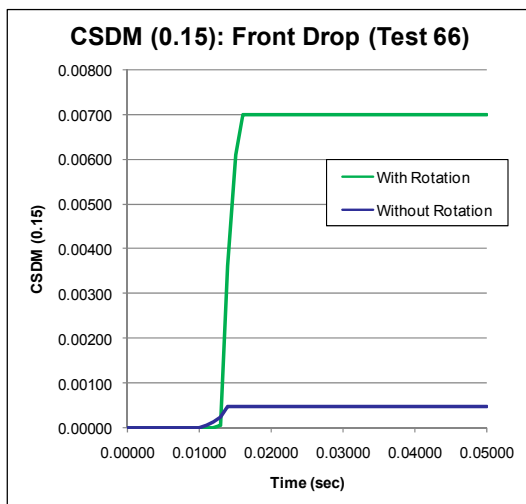
Figure 14. ISO Headform NAP Calculation for Front Drop.

Figure 15 through Figure 16 show the SIMon results for the four drops. SIMon was first run only using the headform center of gravity translational acceleration data. It was then repeated using the CG translational acceleration and the headform rotational velocity calculated by the NAP. In all cases except the crown impact, there was an increase in the CSDM result. However, only the right side impact case showed an increase of the CSDM result near the 50% probability of concussion range. DDM also increased for each hit location, although DDM results approached the threshold for 50% probability of injury. Finally there was a large 41% and 33% increase to the RMDM metric due to rotation. The side impact RMDM was not calculated due to RMDM not being validated for side impacts.



Maximum RMDM	
With Rotation	0.5539
Without Rotation	0.3928
Increase with Rotation	41%

Figure 15. SIMon Results for Front Drop with Rotation



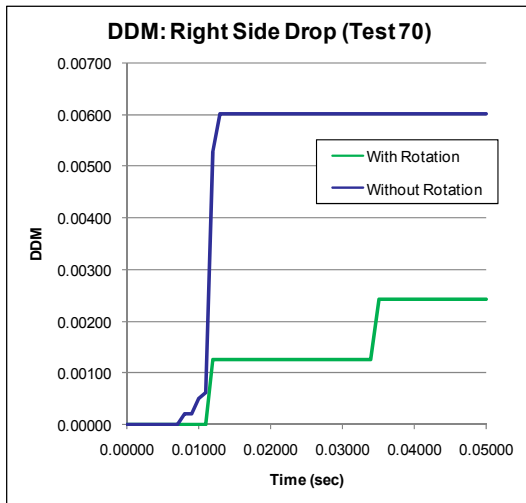


Figure 16. SIMon Results for Right Side Drop with Rotation

DISCUSSION

There are significant differences between the ECE R22 and the FMVSS No. 218 testing methods and pass/fail criteria. FMVSS No. 218 uses a headform constrained to the drop rail traveling at either 6.0 or 5.2 m/sec, against flat and hemispherical anvils respectively. ECE R22 uses a free headform traveling at 7.5 m/sec against both flat and kerbstone anvils. Both standards use resultant peak head acceleration as one of the criterion although FMVSS No. 218 allows peak accelerations up to 400 g while ECE R22 limits the threshold to 275 g. FMVSS No. 218 also uses the time duration of the impact above 150 g and 200 g as pass/fail criteria. ECE R22 uses a HIC36 threshold of 2400.

There was a wide range of correlation values between impact locations in the ECE R22 tests when compared to the FMVSS No. 218 set of experiments (Table 1). The crown had the highest correlation for all injury metric. This is probably due to less rotation, symmetrical loading, a greater surface area on the head interacting with the helmet and the least amount of designed objects on the helmet (visors, etc.) causing different helmet responses. In contrast, the back of the helmet had the lowest correlation coefficient in all cases. Side impacts also had visor mounts which could interfere with the contact dynamics.

The FMVSS No. 218 tests had similar correlation values for all impact directions. This discrepancy between standards could be due to the different dropping mechanisms (one fixed and one free). There could be an effect caused by rotation on the

measured pressures that was unforeseen. The sensors are designed to measure normal forces and special care was taken to reduce all shear forces on the sensors.

As in the FMVSS No. 218 tests, there were a number of side impacts where single or small group of FlexiForce sensors reported very high impact forces. However, Table 1 shows that for ECE tests, there was a lower peak head acceleration needed to cause a 15% probability of skull fracture for side impacts than other impacts. The FMVSS No. 218 data showed that the peak acceleration in side impacts and front impacts are similar but that crown impacts have a lower acceleration limit for 15% probability of skull fracture.

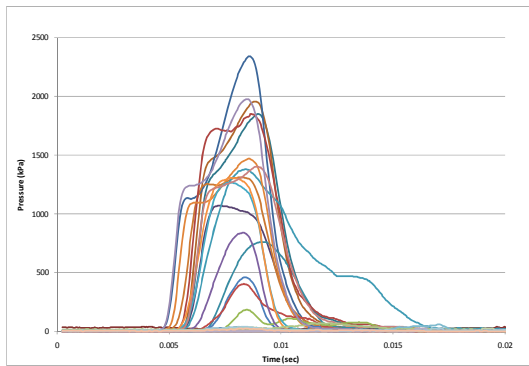
There are a number of factors that complicate the experiments and can cause the discrepancies shown. The helmet visor location and connection point of the visor on the helmet vary among helmets and can cause impacts loads to be distributed differently depending on exact impact location. The loading and rotation of the helmet when impacting a flat or kerbstone anvil can vary against tests on a hemispherical anvil.

The impact loading on the skull can also change due to the contact area between the helmet and the headform. Table 3 shows the average contact surface area for impacts from three different directions.

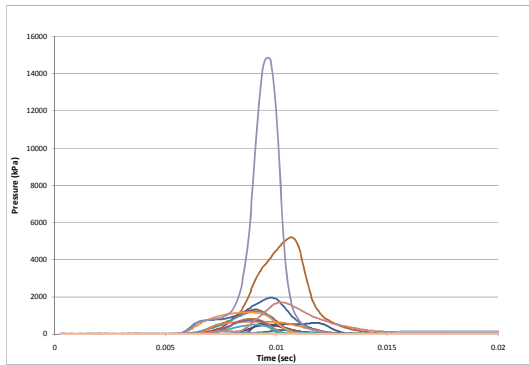
Table 3. Approximate Impact Area According to Location

Impact Direction	Surface Area (cm ²)
Crown	194.6
Front	146.2
Right Side	109.2

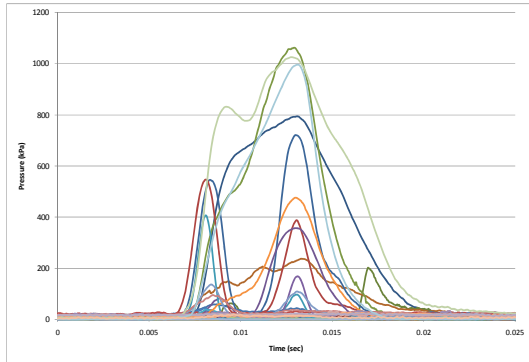
By comparing the contact area for the different impact locations and assuming the total load for each drop will be equal, localized parts of the skull will see nearly twice as much force in side impacts than crown impacts. The figure below shows the FlexiForce pressure traces during a side impact for a distributed and focused loading case. Figure 17a shows the pressure on the scalp distributed over 110 cm² with peak pressures near 2300 kPa. Figure 17b shows a small number of FlexiForce experiencing the loading over a 30 cm² contact area. As a comparison, a typical crown impact is shown in Figure 17c. The peak pressures seen in the crown impact are half of those seen in the side impact (a). The duration of loading is also longer in the crown impact when compared to the side impact, 12 msec duration compared to 7 msec.



Distributed Side Load



Focused Side Load



Distributed Crown Load

Figure 17. Distribution of Load During Impact

As with the FMVSS No. 218 study, the skull fracture analysis results show that peak acceleration is a good indicator for skull fracture, especially if impact orientation is examined. The front, crown and back impacts all had similar correlation trends and the side impacts correlated together. It is when all impacts are correlated together that the R^2 value drops.

The correlation between SFC and skull strain was low ($R^2 = 0.24$) and therefore SFC should not be used as a biofidelic injury metric in this case. The SFC correlate could be significantly off if there were areas of local high pressure on the skull. SFC assumes that forces are applied over the whole impact area and the fractures that occur are linear skull fractures. SFC

will not be able correlate well with peak strains calculated from the FEM under these circumstances.

The adjusted peak head acceleration using peak skull strain as the injury metric should be 278g. This recommended limit is higher than that proposed in the FMVSS No. 218 study (214 g) in Rigby et al. (2009). This could be due to the method of impact (rail constrained head vs. free head) and the difference in shape of the half-head DOT headform and the full-faced ISO headform. As shown in Figure 12, there are significant differences between injury metrics determined using the same helmet but different test protocol and test equipment. The peak accelerations determined using peak strain which correlate with 15% probably of skull fracture are very close to the current ECE R22 peak head acceleration limit of 275 g.

HIC did not correlate well with the most biofidelic skull fracture metric, peak skull strain. It did correlate well with other injury correlates which were also calculated from the headform acceleration trace, SFC and peak head acceleration. The HIC value of 2400 correlates with a peak acceleration value of 261 g. This value also happens to be close to the peak acceleration value at 15% probability of skull fracture (Table 2). Based on peak acceleration limits, the 2400 HIC limit is appropriate. Using the SFC – HIC analysis, the HIC that correlates to 15% probability to skull fracture (2403) is very close to the current HIC criterion of 2400. However, as stated before, HIC is calibrated for the Hybrid III dummy head and not a rigid headform.

The COST 327 study concluded that HIC correlated better with the Abbreviated Injury Scale (AIS) for the head than peak acceleration or impact speed (COST 327 2001). Consistent with previous research, COST 327 found a HIC of 1000 predicted an AIS of 2 and a HIC of 1500 predicted an AIS of 3. It is still unknown what the transfer function (if any) is between a HIC calculated on a Hybrid III and that calculated on an ISO headform.

As shown in the previous FMVSS No. 218 study, only using the translational acceleration of the headform is not adequate for predicting concussion using the SIMon model. The ECE R22 results were very similar to those seen in the FMVSS No. 218 study for CSDM when only translation acceleration was used in the model. Even with a free headform, not accounting for rotation causes a prediction of just 1% probability of concussion. When rotational data is used along with translational acceleration in SIMon, the CSDM value greatly increases, especially for

large angular velocity cases such as side impacts. The right side impact test case showed a CSDM value of 25% which correlates to approximately a 20% chance of concussion. However, for almost every impact in this study, the peak head acceleration was above the published limits for concussion. Given these results, the use of CSDM as calculated in SIMon is not recommended to be used as a measure for concussion.

The Wayne State Tolerance Curve, based on a linear acceleration criterion, predicts a threshold of 60 to 80 g for concussion. Pellman et al. (Pellman, Viano et al. 2003) found the peak acceleration in concussion-causing impacts in professional American football to be 98 ± 28 g. Using small primates data obtained from Ono et al (Ono, Kikuchi et al. 1980) with scaling to humans, Vander Vorst et al. (Vander Vorst, Ono et al. 2007) estimated a 175 g peak linear acceleration limit for 10% probability of concussion. By conducting tests that measure pressure load transmitted to the headform and both translation and angular acceleration of the headform, the injury models can be used to their full potential providing more accurate skull fracture and brain injury predictions.

Thresholds for subdural hematoma injury are usually correlated with rotational acceleration. In order to fully analyze the subdural hematoma, the rotation of the head needs to be measured. A headform integrated with rotational motion sensors, such as a NAP system, should be used. Using PMHS, critical thresholds for injury have been suggested to be 4500 rad/s^2 for durations 15 to 50 msec (Lowenhielm 1974) and 10,000 rad/s^2 for durations under 10 msec (Depreitere, Van Lierde et al. 2006). The right side impact test case using the NAP equipped ISO headform had a peak angular acceleration of 14,400 rad/s^2 . The rotational acceleration was above 10,000 rad/s^2 for 2 msec and above 4,500 rad/s^2 for 4 msec. The ECE R22 test conditions can provide the conditions to produce subdural hematoma.

The ECE R22 and FMVSS No. 218 contusion results are also similar. ECE R22 results suggest a 15% probability of contusion at the current criterion of 275 g peak head acceleration. FMVSS No. 218 reported a 23% probability at 400 g. Both results agree with other real world estimates detailed in the previous FMVSS No. 218 study (COST 327 2001; Vander Vorst, Ono et al. 2007). The trend in the DDM results varied when the rotation was added to the analysis. For some impacts the DDM value increased due to rotation, while in others it decreased. As detailed in the SIMon documentation (Takhounts, Eppinger et

al. 2003), DDM is based on the percentage of the brain tissue experiencing a -100 kPa pressure and undergoing cavitation. It is expected that the addition of rotational data will not overly influence this due to cavitation being primarily linked to translational acceleration. While DDM is less influenced by rotational movement, the fact that DDM values did change given the inclusion of rotational data indicates that drawing conclusions from the DDM values calculated from the drops on the 20 helmets tested in the current study may not be appropriate.

If skull fracture is the primary metric in which a standard would base its pass / fail criteria on, either the rail drop system used by FMVSS No. 218 or the free head drop of ECE R22 are acceptable. Both test methodologies showed peak head acceleration and SFC to correlate highest with skull strain. However, the current study results of ECE R22 tests did show lower correlation between peak head acceleration and SFC to peak strain with R^2 values of 0.52 and 0.39, respectively versus 0.68 and 0.66 in the FMVSS No. 218 study. The R^2 value of 0.52 is low and additional tests using ECE R22 certified helmets could be used for further refinement.

If rotationally induced brain injury metrics are to be considered then a test protocol that allows for headform rotation should be considered. The ECE R22 method will also need to be modified to accept additional NAP sensors on the headform. Otherwise, as demonstrated in this study, there is no benefit to free head drops. All brain injury metrics calculated by SIMon in this and the previous FMVSS No. 218 study were very similar when only the translational acceleration at the CG of the headform is used.

When the results from the same helmets used in the FMVSS No. 218 study were compared to those in the ECE R22 study, there was little correlation between them. The best correlate was peak skull strain followed by peak head acceleration. This is probably due to a number of factors in the way the tests were conducted. The speeds of the FMVSS No. 218 impacts were not consistent between anvils as were the ECE R22 impacts. By having some FMVSS No. 218 impacts at 5.2 m/s and others at 6.0 m/s depending on the anvil being hit, the correlation could be disrupted. The anvil type is also thought to influence the results. It was noted in the FMVSS No. 218 study that hemispherical impacts to the side of the helmet caused local areas of significant high pressure, this in turn then causes a large skull strain. The use of free drops with a fully instrumented headform able to measure angular velocities is

necessary if both skull fracture and brain injury evaluation are of interest.

Limitations The correlation between injury measures based on CG accelerometer data (peak acceleration and SFC) and peak skull strain was quite low compared to the same correlation in the FMVSS No. 218 experiments. However, when broken down into the various impact orientations, the correlation coefficients increased. For the ECE R22 experiments, the side impacts correlations between peak head acceleration and HIC versus peak skull strain was quite different than that of the other impact orientations. This is seen by the low injury metric values for 15% probability of skull fracture in Table 1. For the FMVSS No. 218 study, the crown impacts had injury metrics for 15% probability of skull fracture at lower values compared to other impact sites.

CONCLUSION

The biofidelity of the injury criteria used by ECE R22 were examined against biomechanically based injury metrics. Helmet drop tests were conducted using the ECE R22 protocol to obtain acceleration and pressure data on the headform during impact attenuation tests. The data was used in finite element models to predict injuries for skull fracture, concussion, brain contusion, and subdural hematoma. The predicted damage measures were then correlated against the injury criteria used in ECE R22 (peak head acceleration and HIC). Below are a summary of the findings from this research:

- Peak head acceleration was the best correlate to skull fracture injury measures identified in this study. HIC was only a good correlate to other acceleration based injury metrics.
- The current ECE R22 linear acceleration limit of 275 g is slightly higher than the calculated thresholds of injury used in this study for skull fracture, 252 g for 15% probability of skull fracture.
- ECE R22 tests with NAP instrumentation allowing for assessment of translational and rotational movement of the headform and subsequent SIMon analysis with and without rotational movement indicates that to evaluate brain injury measures in the ECE R22 protocol, both rotational and translational movement of the headform needs to be collected.
- While the FMVSS No. 218 method of helmet evaluation gives differing results when compared to ECE R22 tests, both testing methods show that peak head acceleration is the best correlate

to skull strain. Both standards demonstrate that by using an appropriate threshold of peak head acceleration, skull fracture can be protected against.

ACKNOWLEDGEMENTS

This study was funded by NHTSA through an interagency agreement (DTNH22-07-X-00073) with the U.S. Army Medical Research and Materiel Command (MRMC) under contract W81XWH-06-C-0051. The previous study evaluating the biofidelity of FMVSS No. 218 (Rigby et al., 2009) was also funded by NHTSA through an Interagency Agreement with the U.S. Army MRMC. The views expressed in both papers are those of the authors and do not represent the views of NHTSA.

REFERENCES

- Chan, P., Z. Lu, P. Rigby, E. Takhounts, J. Zhang, N. Yoganandan and F. Pintar (2007). Development of Generalized Linear Skull Fracture Criterion. 20th International Technical Conference on the Enhanced Safety of Vehicles, Lyon, France.
- COST 327 (2001). COST 327, Motorcycle Safety Helmets. B. Chinn, European Commission.
- Depreitere, B., C. Van Lierde, J. V. Sloten, R. Van Audekercke, G. Van der Perre, C. Plets and J. Goffin (2006). "Mechanics of acute subdural hematomas resulting from bridging vein rupture." J Neurosurg, **104**(6): 950-6.
- Hodgson, V. and L. Thomas (1971). Breaking strength of the human skull vs. impact surface curvature., Wayne State University.
- Hodgson, V. and L. Thomas (1973). Breaking strength of the human skull vs. impact surface curvature., Wayne State University.
- Khalil, T. and R. Hubbard (1977). "Parametric Study of Head Response by Finite Element Modeling." J. Biomechanics **10**: 119-132.
- Lowenhielm, P. (1974). "Dynamic properties of the parasagittal bridging veins." Z Rechtsmed. **74**(1): 55-62.
- Newman, J. (1980). Head Injury Criteria in Automotive Crash Testing. 24th Stapp Car Crash Conference. Troy, Michigan, USA, Society of Automotive Engineers, Inc.: 703-747.
- NHTSA (2007). Motorcycle Helmet Use Laws. Traffic Safety Facts, National Highways Traffic Safety Administration.

- NHTSA (2008). "Consumer Information; New Car Assessment Program." Federal Register **73**(14): 4006-50.
- NHTSA (2009). Motorcycle Helmet Use in 2009 - Overall Results. Traffic Safety Facts, National Highways Traffic Safety Administration.
- NIH (2000). Visible Human Project. Bethesda, Maryland, National Library of Medicine.
- Ono, K., A. Kikuchi, M. Knakamura, H. Kobayashi and N. Nakamura (1980). "Human head tolerance to sagittal impact reliable estimation deduced from experimental head injury using subhuman primates and human cadaver skulls." Stapp Car Crash Journal: 105-160.
- Pellman, E. J., D. C. Viano, A. M. Tucker, I. R. Casson and J. F. Waeckerle (2003). "Concussion in professional football: reconstruction of game impacts and injuries." Neurosurgery. **53**(4): 799-812; discussion 812-4.
- Takhounts, E. G., R. H. Eppinger, J. Q. Campbell, R. E. Tannous, E. D. Power and L. S. Shook (2003). On the development of the SIMon finite element head model. Proceedings of the 47th Stapp Car Crash Conference, San Diego, California, USA.
- UNECE R.22 (2000). Regulation No. 22. www.unece.org/trans/main/wp29/wp29regs21-40.html
- Economic Commission for Europe.
- Vander Vorst, M., P. Chan, J. Zhang, N. Yoganandan and F. Pintar (2004). "A new biomechanically-based criterion for lateral skull fracture." Annu Proc Assoc Adv Automot Med. **48**: 181-95.
- Vander Vorst, M., K. Ono, P. Chan and J. Stuhmiller (2007). "Correlates to traumatic brain injury in nonhuman primates." J Trauma. **62**(1): 199-206.
- Vander Vorst, M. J. and P. Chan (2004). Biomechanically-based criterion for lateral skull fracture. 48th Annual Proceedings of the Association for the Advancement of Automotive Medicine.
- Vander Vorst, M. J., J. H. Stuhmiller, K. Ho, N. Yoganandan and P. F. (2003). Statistically and biomechanically based criterion for impact-induced skull fracture. 27th Annual Proceedings of the Association for the Advancement of Automotive Medicine. Lisbon, Portugal.
- Wood, J. (1971). "Dynamic response of human cranial bone." J Biomech **4**(1): 1-12.
- Zhang, J., N. Yoganandan, F. A. Pintar and T. A. Gennarelli (2006). "Role of translational and rotational accelerations on brain strain in lateral head impact." Biomed Sci Instrum. **42**: 501-6.